

Mobility of Long-Lived Fullerene Radical in Solid State and Nonlinear Temperature Dependence

Yoko Abe,^{†,‡} Hideyuki Tanaka,[†] Yunlong Guo,[†] Yutaka Matsuo,^{*,†} and Eiichi Nakamura^{*,†}

[†]Department of Chemistry, The University of Tokyo, 7-3-1 Hongo, Bunkyo-ku, Tokyo 112-0033, Japan

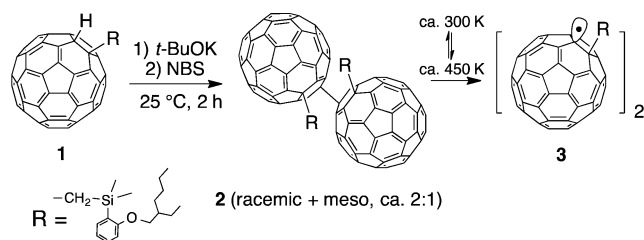
[‡]Mitsubishi Chemical Group Science and Technology Research Center, Inc., 1000 Kamoshida, Aoba-ku, Yokohama, Kanagawa, 227-8502, Japan

S Supporting Information

ABSTRACT: A singly bonded fullerene dimer $[C_{60}R]_2$ in the solid state thermally generates a pair of fullerene radicals $C_{60}R^\bullet$ that dissociate reversibly and irreversibly upon heating and cooling of the solid. The temperature dependence of the electron mobility of the solid shows striking nonlinearity, caused by the dissociation of a strongly interacting radical pair into two free radicals, which interact with the neighboring fullerene molecules to increase the mobility 10 times to a value of $1.5 \times 10^{-3} \text{ cm}^2 \text{ V}^{-1} \text{ s}^{-1}$. The nonlinearity is due to the plastic crystalline nature of fullerene crystals.

A challenge in organoelectronic research is to control the behavior of organic molecules in the solid state. In this study, we focused on the solid-state property of a singly bonded [60]fullerene dimer $(C_{60}R)_2$ that generates a radical pair $(RC_{60}^\bullet)_2$ through thermal homolytic cleavage of the central C–C bond (Scheme 1).^{1–5} What intrigued us was the propensity

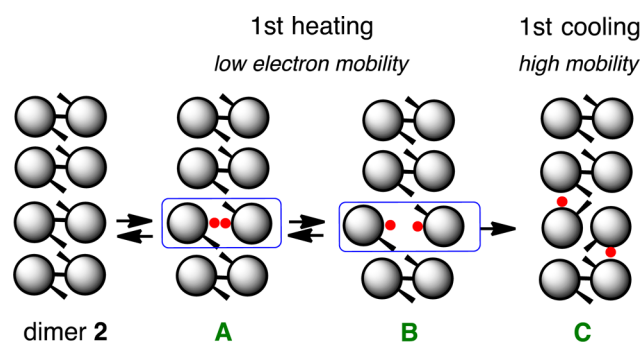
Scheme 1. Synthesis of Fullerene Dimer 2 and Thermal C–C Bond Dissociation in Solid State



of fullerenes in solid to form plastic crystals, in which a short-range orientational order of the fullerene radical pair may change thermally without affecting the long-range translational order.^{6,7}

Herein, we report on a striking nonlinear temperature dependence of the radical concentration and the electron mobility that can be ascribed to this property of fullerene crystals. Thus, heating of a microcrystalline powder of 2 up to $\sim 450 \text{ K}$ generated a strongly and weakly interacting radical pair A and B at a concentration of 0.01% at 400 K (Scheme 2), which, upon cooling, underwent irreversible reorientation to generate free radicals C. This caused a sudden 10-fold increase in the electron mobility of the solid. The radicals act as a

Scheme 2. Four Probable States during Conversion of Dimer 2 to Two Radicals^a



^aIn the final state, the radicals act as a dopant of the dimer solid and increase the electron mobility.

dopant of the dimer solid. The free radicals are stable during repeated heating/cooling and for $>1000 \text{ min}$ without decay under nitrogen. The whole process occurs with little change of the crystal lattice pattern. The dimer in solution exists as aggregates and shows a similar nonlinear behavior. The present work will provide new insights into organic spin-electronic devices^{8–11} and fullerene-based carrier transport materials.¹²

The dimer 2 $[C_{60}\{\text{CH}_2\text{SiMe}_2(\text{C}_6\text{H}_4(2\text{-ethylhexyloxy})-2)\}]_2$ has two branched alkyl chains that increase the solubility. It was synthesized in 96% yield from hydro(dimethyl(2-ethylhexyloxyphenyl)silylmethyl)[60]fullerene 1 that is readily available in 93% yield from [60]fullerene (Scheme 1).¹³ The dimer, especially in its pure recrystallized form, is rather insoluble in a variety of solvents, and exists predominantly as aggregates. Dynamic laser light scattering (DLS) analysis of a 1,2-dichlorobenzene solution (Supporting Information (SI)) revealed the presence of aggregates of several nanometers to micrometers in size at different concentrations (3 mM and 3 μM) and temperatures (300 and 363 K).

Cyclic voltammetric analysis of the dimer 2 in 1,2-dichlorobenzene containing $\text{Bu}_4\text{N}^+\text{ClO}_4^-$ is in accord with the formation of a radical pair, as previously reported^{3a} (Figure 1). One cathodic peak, two pairs of reversible redox waves, and one anodic peak were observed. The first cathodic peak at -1.20 V vs Fc/Fc^+ corresponds to the reduction of 2 causing

Received: January 20, 2014

Published: February 18, 2014

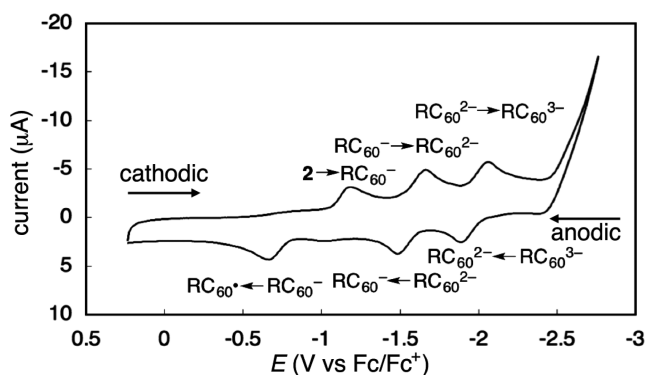


Figure 1. Cyclic voltammogram of **2**. Measurement performed in a 0.3 mM 1,2-dichlorobenzene solution containing $\text{Bu}_4\text{N}^+\text{ClO}_4^-$ (0.1 M) as supporting electrolyte at 298 K with a scan rate of 0.1 V/s. Glassy carbon, platinum wire, and Ag/Ag^+ electrodes were used as the working, counter, and reference electrodes, respectively. The second and third half-wave reduction potentials ($E_{1/2}^{\text{red}2}$ and $E_{1/2}^{\text{red}3}$) were -1.57 and -1.97 V, respectively.

dissociation into two molecules of RC_{60}^- , and the two remaining reduction peaks are assigned to RC_{60}^- to RC_{60}^{2-} and RC_{60}^{2-} to RC_{60}^{3-} . On the anodic scan, the two reversible anodic peaks are due to oxidation of the tri- and dianions back to RC_{60}^- , and the last irreversible anodic peak at -0.67 V is due to oxidation of RC_{60}^- to RC_{60}^\bullet ,¹⁴ which then undergoes rapid recombination to regenerate the dimer **2**. The data indicates that the monomeric radical RC_{60}^\bullet has higher electron affinity than the dimer, and suggests that, if generated in the solid of the dimer, the free radical may act as a dopant and increase the electron mobility of the solid.

The structure of the dimer was determined by X-ray crystallographic analysis of a single crystal grown in chloroform (Figure 2a,b). The inter-fullerene C–C bond distance is 0.152(1) nm. We noted that the *meso* and *racemo* molecules crystallize together without greatly affecting the translational order of the crystal, where the side chains are located among the fullerene moieties. X-ray diffraction (XRD) analysis of a powder sample at 298–453 K, and then at 298 K after cooling, showed that molecular packing is not greatly affected by the heating except for the disappearance of a few peaks seen at 298 K in the small angle region, corresponding to the fullerene packing (8.8–17.7 Å) (Figure 2c).

In agreement with the XRD data, DSC analysis showed subtle signs of thermal events that occur during heating and cooling (Figure 2d). Heating caused two-phase transitions at ~ 345 and ~ 400 K with small exothermicity, and cooling after melting (~ 540 K) showed a small exothermic phase transition at ~ 430 K.

The electron spin resonance (ESR) spectra of the dimer **2** in a microcrystalline powder showed an intriguing nonlinear phenomenon (Figure 3a). The enthalpy change was studied from the slope of the van't Hoff plot in which $\ln(T \times \text{intensity})$ is plotted against $1000/T$.^{1b} The ESR signal intensity increased between room temperature and 362 K with a small slope of the van't Hoff plot ($\Delta H = 2.3$ kcal/mol, Table 1), and above ~ 360 K (cf. a phase transition observed by DSC at a similar temperature), it increased sharply up to 440 K ($\Delta H = 22.0$ kcal/mol). The spin concentration at 400 K was determined to be 7.4×10^{-8} mol/g by comparison of the signal intensity of the radical with that of the signal of 4-hydroxy-2,2,6,6-tetramethylpiperidine-1-oxyl (TEMPO) (SI), i.e., 0.01 mol

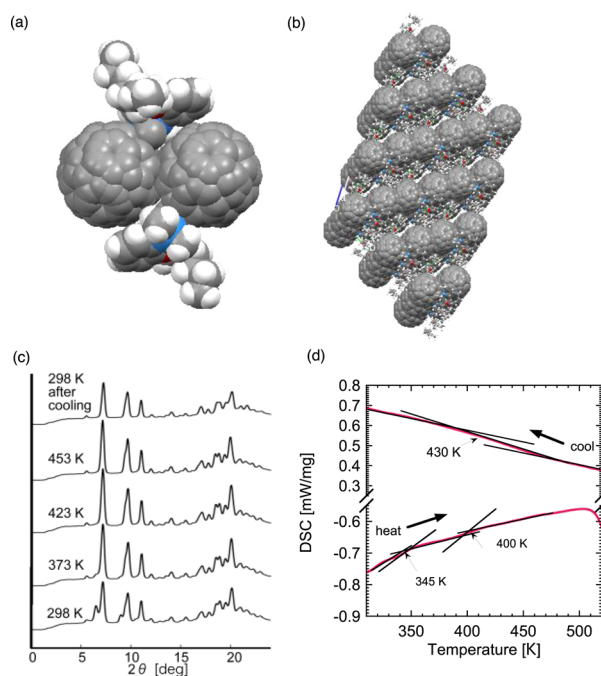


Figure 2. Single-crystal X-ray structure of $2 \cdot (\text{CHCl}_3)$, and XRD and DSC data for a microcrystalline powder obtained by precipitation from 1,2-dichlorobenzene. (a) Side view of space-filling model. (b) Crystal-packing structure. The crystal is monoclinic, space group = $P\bar{1}$, $a = 10.014$ Å, $b = 15.869$ Å, $c = 17.702$ Å, $\alpha = 112.97^\circ$, $\beta = 92.59^\circ$, $\gamma = 105.99^\circ$, $V = 2452.48$ Å³, R (2σ cutoff) = 13.66%. Fullerene cores are structurally disordered due to the mixture of *meso* and *racemo* isomers. Chloroform is omitted for clarity. (c) XRD pattern at various temperatures. (d) DSC data for heating (bottom) of the microcrystalline powder and cooling (top) after melting.

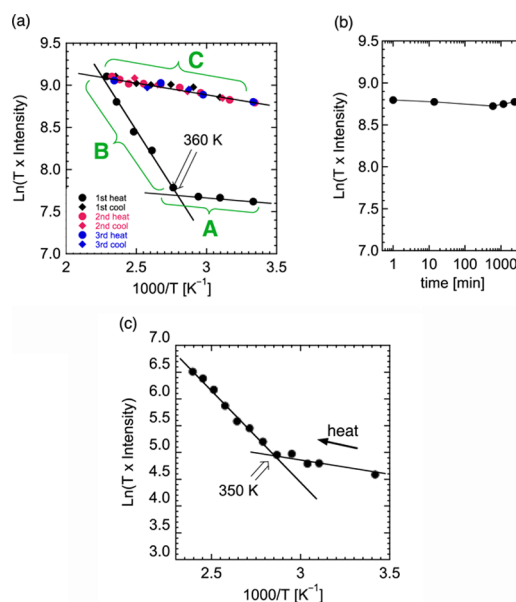


Figure 3. van't Hoff plot of the ESR signal intensity of **2**. (a) Measurement of a microcrystalline powder at various temperatures. (b) Long-time measurement of the solid at room temperature after the first cooling. (c) Measurement in 1,2-dichlorobenzene. The g -factors are 2.0023 in solution and 2.0025 in solid (Figure S2), in agreement with that reported value for RC_{60}^\bullet ($\text{R} \cong \text{CH}_2\text{PO}(\text{OEt})_2$, $g = 2.0023$).^{3a}

% radical concentration in the dimer solid (Figure S2). Cooling of the heated sample from 440 K to room temperature resulted

Table 1. Enthalpy of Dissociation of Dimer 2 (kcal/mol) in Solid and in Solution, As Calculated from the van't Hoff Plots in Figure 3a,c

state	measurement	$-\Delta H$	temp/K
solid	1st heating	2.3	300–362
	1st heating	22.0	362–440
	1st cooling	2.4	440–300
	2nd heating	2.4	300–440
	2nd cooling	2.7	440–300
	3rd heating	2.3	300–440
	3rd cooling	2.1	300–440
solution	1st heating	6.1	293–340
	1st heating	28.2	350–420
	2nd heating	8.7	293–360
	2nd heating	30.2	370–420

in an unexpected consequence. The spin concentration decreased very slowly ($\Delta H = 2.4$ kcal/mol) and remained high, even after heating and cooling for the second and the third times, where exactly the same van't Hoff plots were obtained (Figure 3a). One possible reason for this sudden change is a phase transition from an overheated state involving equilibrating radical pairs (A and B) to a second state involving a free radical (C). The radical concentration after cooling remained constant for well over 1000 min (Figure 3b), indicating that this second state is structurally stable.

Upon consideration of the XRD and DSC data, and ESR temperature dependence of the solid dimer, we consider that the radical pair maintains strong interaction within the pair up to ~ 360 K (cf. A), dissociates reversibly into two weakly interacting radicals above this temperature (B), and then at a certain temperature around 400 K (cf. DSC) the two radicals start to change their molecular orientation (C), perhaps accompanying a small change of local translational order as suggested by the disorder found in a single crystal.

The ESR spectra of the dimer 2 in solution (1,2-dichlorobenzene) also showed a nonlinear behavior (Figure 3c and Table 1) similar to in the low temperature region of the first heating of the solid sample (Figure 3a). As shown in Figure 3c, the intensity of the ESR signal increased between room temperature and 340 K with a small slope ($\Delta H = 6.1$ kcal/mol) and sharply between 350 and 420 K ($\Delta H = 28.2$ kcal/mol). Essentially the same data were obtained upon second heating (Table 1, bottom), indicating that there is little memory of thermal history in solution. This can be rationalized by the structural mobility of the micrometer-size aggregates. The spin concentration at 400 K was 7.2×10^{-8} mol/g, a value almost identical to one in solid. In light of the DLS information above and the similarity of this ESR profile to that of the solid at low temperatures, we consider that the solution properties of the dimer reflect that of aggregates rather than a unimer.

The electron mobility of the solid dimer exhibited even more pronounced nonlinear temperature dependence than the one found in the van't Hoff plot. A bottom-gate field effect transistor (FET) device made of 2 (spin-coated as a CS_2 solution) exhibited a typical FET property (Figure 4a). The electron mobility on the first heating to 470 K remained rather constant, in a $(0.1\text{--}0.3) \times 10^{-3} \text{ cm}^2 \text{ V}^{-1} \text{ s}^{-1}$ range, and peaking slightly at 330 and 390 K. In light of the van't Hoff plot in the same temperature range (Figure 3a), we consider that the low mobility recorded here is because the radical pairs (A and B) do

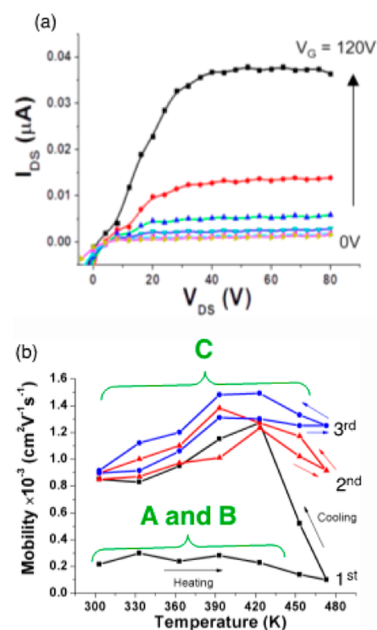


Figure 4. (a) Output curves of the FET device at 420 K. (b) Temperature dependency of electron mobility of 2 in the solid state.

not have strong electronic interactions with the neighboring fullerene molecules.

It was most remarkable that cooling from 470 to 420 K caused an almost 10-fold increase of the mobility to $1.2 \times 10^{-3} \text{ cm}^2 \text{ V}^{-1} \text{ s}^{-1}$, while further cooling to room temperature decreased the mobility only to $0.85 \times 10^{-3} \text{ cm}^2 \text{ V}^{-1} \text{ s}^{-1}$. Such an increase in the mobility suggests that the fullerene radicals started to affect the bulk property of the solid upon cooling. In light of the van't Hoff plot and the high radical concentration at the first cooling (Figure 3a), we consider that the emergence of the free radical C caused by irreversible orientational change of the fullerene moiety is responsible for the increased electron mobility.

In the second heating/cooling cycle, the mobility peaked at $1.4 \times 10^{-3} \text{ cm}^2 \text{ V}^{-1} \text{ s}^{-1}$. The third heating/cooling cycle followed similar traces, peaking at $1.5 \times 10^{-3} \text{ cm}^2 \text{ V}^{-1} \text{ s}^{-1}$. In agreement with the ESR evidence of the persisting radical, the second state of the dimer solid involving C is structurally stable and maintains a high level of mobility for >1000 min (after the first heating/cooling cycle the FET device was kept for 300 K; SI).

In summary, we found that thermolysis of the solid fullerene dimer 2 results in reversible and irreversible generation of radicals 3. The free radicals C irreversibly generated after the first cooling of the solid do not recombine because of the emergence of a second state of molecular packing, which produces a solid containing a long-lived radical. This free radical acts as a dopant for the fullerene solid and increases the electron mobility. On the other hand, radical pairs A and B maintain strong interactions with each other and do not interact electronically with the neighboring fullerene molecules, and hence do not increase the mobility of the solid. The processes of the formation of the radicals display an unusual nonlinear temperature dependence on the radical concentration and the electron mobility. This can be ascribed to the intrinsic tendency of fullerene molecules to form plastic crystals, where the fullerene molecules can change their orientation with low

activation energy without affecting the long-range translational order of the crystal.

■ ASSOCIATED CONTENT

■ Supporting Information

Synthetic procedures, ESR spectra, details of FET data, and crystallographic data (CIF). This material is available free of charge via the Internet at <http://pubs.acs.org>.

■ AUTHOR INFORMATION

Corresponding Authors

matsuo@chem.s.u-tokyo.ac.jp

nakamura@chem.s.u-tokyo.ac.jp

Notes

The authors declare no competing financial interest.

■ ACKNOWLEDGMENTS

We thank Dr. Chao Liu for technical assistance and Dr. Sobi Asako for helpful discussion on the data analysis. This work was generously supported by the Funding Program for Next-Generation World-Leading Researchers (Y.M.), Strategic Promotion of Innovative Research, the Specially Promoted Research Grant (KAKENHI 22000008 to E.N.), Grant-in-Aid for Young Scientists (B) (No. 24750177) from MEXT and the Japan Science and Technology Agency (JST).

■ REFERENCES

- (1) (a) Morton, J. R.; Preston, K. F.; Krusic, P. J.; Wasserman, E. *J. Chem. Soc., Perkin Trans. 2* **1992**, 1425. (b) Morton, J. R.; Preston, K. F.; Krusic, P. J.; Hill, S. A.; Wasserman, E. *J. Am. Chem. Soc.* **1992**, *114*, 5454. (c) Fagan, P. J.; Krusic, P. J.; McEwen, C. N.; Lazar, J.; Parker, D. H.; Horrn, N.; Wasserman, E. *Science* **1993**, *262*, 404.
- (2) Segura, J. L.; Martin, N. *Chem. Soc. Rev.* **2000**, *29*, 13.
- (3) (a) Cheng, F.; Murata, Y.; Komatsu, K. *Org. Lett.* **2002**, *4*, 2541. (b) Wang, G.-W.; Wang, C.-Z.; Zhua, S.-E.; Murata, Y. *Chem. Commun.* **2011**, *47*, 6111.
- (4) Lu, S.; Jin, T.; Kwon, E.; Bao, M.; Yamamoto, Y. *Angew. Chem., Int. Ed.* **2012**, *51*, 802.
- (5) (a) Konarev, D. V.; Khasanov, S. S.; Otsuka, A.; Saito, G. *J. Am. Chem. Soc.* **2002**, *124*, 8520. (b) Matsuo, Y.; Nakamura, E. *J. Am. Chem. Soc.* **2005**, *127*, 8457. (c) Xiao, Z.; Matsuo, Y.; Maruyama, M.; Nakamura, E. *Org. Lett.* **2013**, *15*, 2176.
- (6) *Carbon Molecules and Materials*; Setton, R., Bernier, P., Lefrant, S., Eds.; Taylor & Francis: New York, 2002.
- (7) Li, C.-Z.; Matsuo, Y.; Nakamura, E. *J. Am. Chem. Soc.* **2010**, *132*, 15514.
- (8) (a) Nakahara, K.; Iwasa, S.; Satoh, M.; Morioka, Y.; Iriyama, J.; Suguro, M.; Hasegawa, E. *Chem. Phys. Lett.* **2002**, *359*, 351. (b) Nishide, H. *Electrochim. Acta* **2004**, *50*, 827. (c) Nishide, H.; Oyaizu, K. *Science* **2008**, *319*, 737. (d) Suga, T.; Ohshiro, H.; Sugita, S.; Oyaizu, K.; Nishide, H. *Adv. Mater.* **2009**, *21*, 1627. (e) Morita, Y.; Suzuki, S.; Sato, K.; Takui, T. *Nat. Chem.* **2011**, *3*, 197. (f) Morita, Y.; Nishida, S.; Murata, T.; Moriguchi, M.; Ueda, A.; Satoh, M.; Arifuku, K.; Sato, T.; Fujii, T. *Nat. Mater.* **2011**, *10*, 947.
- (9) (a) Kubo, T.; Shimizu, A.; Sakamoto, M. *Angew. Chem., Int. Ed.* **2005**, *44*, 6564. (b) Chikamatsu, M.; Mikami, T.; Chisaka, J.; Yoshida, Y.; Azumi, R.; Yase, K.; Shimizu, A.; Kubo, T.; Morita, Y.; Nakasuji, K. *Appl. Phys. Lett.* **2007**, *91*, 043506. (c) Kurata, T.; Koshika, K.; Kato, F.; Kido, J.; Nishide, H. *Chem. Commun.* **2007**, 2986.
- (10) Kishimoto, Y.; Abe, J. *J. Am. Chem. Soc.* **2009**, *131*, 4227.
- (11) Namai, H.; Ikeda, H.; Hoshi, Y.; Kato, N.; Morishita, Y.; Mizuno, J. *J. Am. Chem. Soc.* **2007**, *129*, 9032.
- (12) (a) Shibata, K.; Kubozono, Y.; Kanbara, T.; Hosokawa, T.; Fujiwara, A.; Ito, Y.; Shinohara, H. *Appl. Phys. Lett.* **2004**, *84*, 2572. (b) Kusai, H.; Nagano, T.; Imai, K.; Kubozono, Y.; Sako, Y.; Takaguchi, Y.; Fujiwara, A.; Akima, N.; Iwasa, Y.; Hino, S. *Appl. Phys. Lett.* **2006**, *88*, 173509. (c) Kawasaki, N.; Nagano, T.; Kubozono, Y.; Sako, Y.; Morimoto, Y.; Takaguchi, Y.; Fujiwara, A.; Chu, C.-C.; Imae, T. *Appl. Phys. Lett.* **2007**, *91*, 243515. (d) Ullah, M.; Singh, T. B.; Sitter, H.; Sariciftci, N. S. *Appl. Phys. A: Mater. Sci. Process.* **2009**, *97*, 521. (e) Ball, J. M.; Bouwer, R. K. M.; Kooistra, F. B.; Frost, J. M.; Qi, Y.; Domingo, E. B.; Smith, J.; de Leeuw, D. M.; Hummelen, J. C.; Nelson, J.; Kahn, A.; Stingelin, N.; Bradley, D. D. C.; Anthopoulos, T. D. *J. Appl. Phys.* **2011**, *110*, 014506.
- (13) (a) Matsuo, Y.; Iwashita, A.; Abe, Y.; Li, C. Z.; Matsuo, K.; Hashiguchi, M.; Nakamura, E. *J. Am. Chem. Soc.* **2008**, *130*, 15429. (b) Matsuo, Y.; Sato, Y.; Niinomi, T.; Soga, I.; Tanaka, H.; Nakamura, E. *J. Am. Chem. Soc.* **2009**, *131*, 16048. (c) Tanaka, H.; Abe, Y.; Matsuo, Y.; Kawai, J.; Soga, I.; Sato, Y.; Nakamura, E. *Adv. Mater.* **2012**, *24*, 3521. (d) Matsuo, Y.; Oyama, H.; Soga, I.; Okamoto, T.; Tanaka, H.; Saeki, A.; Seki, S.; Nakamura, E. *Chem. Asian J.* **2013**, *8*, 121.
- (14) Matsuo, Y.; Kuninobu, Y.; Muramatsu, A.; Sawamura, M.; Nakamura, E. *Organometallics* **2008**, *27*, 3403.